CO_2 Sequestration and Recycle by Photosynthesis

Annual Report

Reporting Period Start Date: Oct. 1, 2001
Reporting Period End Date: Sept. 30, 2002

Dr. Steven S. C. Chuang

Date Report was Issued (Feb. 2003)

DOE Award Number: DE-FG26-01NT41294

Department of Chemical Engineering
The University of Akron
Akron, OH 44325-3906

ABSTRACT

Visible light-photocatalysis could provide a cost-effective route to recycle CO_2 to useful chemicals or fuels. Research is planned to study the reactivity of adsorbates, their role in the photosynthesis reaction, and their relation to the nature of surface sites during photosynthesis of methanol and hydrocarbons from CO_2/H_2O over four types of MCM-41/Al_2O_3-supported TiO_2 and CdS catalysts: (i) ion-exchanged metal cations, (ii) highly dispersed cations, (iii) monolayer sites, and (iv) modified monolayer catalysts. TiO_2 was selected since it has exhibited higher activity than other oxide catalysts; CdS was selected for its photocatalytic activity in the visible light region. Al_2O_3 provides excellent hydrothermal stability. MCM-41 offers high surface area (more than 800 m^2/g), providing a platform for preparing and depositing a large number of active sites per gram catalyst. The unique structure of these ion exchange cations, highly dispersed cations, and monolayer sites provides an opportunity to tailor their chemical/coordination environments for enhancing visible-light photocatalytic activity and deactivation resistance. The year one research tasks include (i) setting up experimental system, (ii) preparing ion-exchanged metal cations, highly dispersed cations, monolayer sites of TiO_2 and CdS, and (iii) determination of the dependence of methanol activity/selectivity on the catalyst preparation techniques and their relation to adsorbate reactivity. During the first quarter, we have purchased a Gas Chromatography and all the necessary components for building 3 reactor systems, set up the light source apparatus, and calibrated the light intensity. In addition, monolayer TiO_2/MCM-41 and TiO_2/Al_2O_3 catalyst were prepared. TiO_2/Al_2O_3 was found to exhibit high activity for methanol synthesis. Repeated runs was planned to insure the reproducibility of the data.

TABLE OF CONTENTS

LIST OF GRAPHICAL MATERIALS

INTRODUCTION

CO_2 emission has become a worldwide problem due to its potential impact on global climate. One promising alternative to these technologies is artificial photosynthesis. There has been much on-going research to develop photochemical processes that can activate thermodynamically stable molecules, i.e., CO_2, H_2O, and CH_4, and convert them to CH_3OH or other valuable chemicals (1-10). Most of these studies have utilized ultraviolet (UV) light to activate the catalyst; the reaction processes have suffered from low efficiencies, catalyst instability, and deactivation. Additionally, the required use of UV light to excite valence electrons makes the process prohibitively expensive for the utilization of CO_2 as a feedstock for the synthesis of chemicals and fuels.

A practical and effective photocatalyst for the CO_2/H_2O reaction must possess: (i) the ability to excite valence electrons with visible light, (ii) a high activity/selectivity toward CH_3OH and hydrocarbons, and (iii) catalyst stability. No catalyst has been identified that exhibits both promising activity and stability during photosynthesis of CO_2 and H_2O to form CH_3OH or CH_4. The key to developing an efficient catalyst to utilize visible light lies in our understanding of the reaction mechanism, which will provide a scientific basis for catalyst design. The objectives of this research are to (i) develop a fundamental understanding of the reactivity of adsorbates, the nature of surface sites, and their corresponding reactivity, (ii) improve deactivation resistance, and (iii) control catalyst activity/stability through the manipulation of the sites' coordination/chemical environment. The overall goal of this research is to provide a greater predictive capability for the design of visible light-photosynthesis catalysts by a deeper understanding of the reaction kinetics and mechanism as well as by better control of the coordination/chemical environment of active sites.

EXECUTIVE SUMMARY

The key accomplishments of the year 1 research include (i) setting in situ infrared photocatalytic reactor, (ii) preparation of monolayer TiOx catalysts, and (iii) demonstration the effectiveness of monolayer TiOx catalyst for the conversion of CO_2 and H_2O to methane and methanol. Year 2 research will focus on catalyst screening, search for the effective promoter, support, and active catalyst.

EXPERIMENTAL

IR Reactors

Two different in situ IR reactors were utilized in these studies: a general reactor capable of handling most gas-solid or liquid-solid reactions and a specialized reactor designed for photocatalysis in particular. The general reactor, which is shown in Fig. 1, is of stainless steel construction and contains a hollow cylinder through the entire body 10 mm in diameter and 85 mm in length. The purpose of the hollow cylinder is to house two CaF_2 rods. The rods are inserted from both ends of the reactor and meet in the center, where the catalyst disk is placed. These CaF_2 rods serve two functions: (i) to allow the IR beam to pass into the reactor and through the catalyst disk with a transmission range of 4000 to 1200 cm^{-1} and (ii) to eliminate dead space within the reactor. The reactor is closed at both ends by a screw-on flange which forms a seal with a disk-like CaF_2 window that fits into a specially machined groove. The reactor also contains a thermowell where a K-type thermocouple is inserted such that its tip touches the top of the catalyst disk. For high-temperature applications, the reactor is wrapped with Barnstead Thermolyne standard insulated samox heating tape. Additional insulation is also added after the heating tape has been properly wrapped. The thermocouple and heating tape are connected to an Omega temperature controller (model #CN2011) capable of operating in a ramp and soak mode for temperature control. Inlet and outlet ports for cooling water are also located on the reactor to prevent the O-rings from melting and to expedite the cooling process when

necessary. The reactor allows monitoring the interactions of catalyst precursors with the Al-MCM-41 and Al_2O_3 surfaces and determining the catalyst surface properties by infrared spectra of adsorbed CO.

The photoreactor is similar to the general high-pressure reactor, but possesses some very unique features that suit in situ study of photocatalytic reactions. A 3-D representation of the photoreactor is shown in Fig. 2. This reactor is also constructed of stainless steel. The body of the reactor is a hollow cube equipped with two thin rectangular pieces of steel welded diagonally across from each other within the cube. These squares serve to support the catalyst holder at approximately a 60° angle with respect to the bottom of the cube. A top view and side view are shown in Figs. 3 and 4, respectively. The catalyst holder, shown in Fig. 5, holds the catalyst in place such that it is exposed to both the IR beam and the radiation used to initiate the photocatalytic reaction. Tubing, which houses thallium bromoiodide rods, has been welded at opposite ends of the cube and in turn connects to flanges that house thallium bromoiodide windows. These rods and windows allow the IR beam to pass into the reactor, through the catalyst disk, and out of the reactor into the detector. Thallium bromoiodide was chosen because it allows IR transmission over the range 400-4000 cm^{-1}. A flange is also attached to the top of the reactor which houses a large CaF_2 window. This window allows UV and visible light to pass into the reactor and onto the catalyst disk. The reactor is of course also equipped with inlet and outlet lines which are located on the sides of the cube normal with respect to the tubing which houses the rods. Finally, because of the small size of the catalyst disk, it was necessary to construct a means by which more catalyst could be exposed to the light in order to increase conversion. This was accomplished by machining a small shelf just below the CaF_2 window that secures a donut-shaped aluminum container which in turn is capable of holding a few hundred

milligrams of additional catalyst. Although this additional catalyst is not subjected to IR, it is in the path of the UV/visible light radiation and therefore is active in the conversion of CO_2 and H_2O. This additional conversion will aid in product analysis by increasing product concentration. This reactor is capable of operating at high pressures and temperatures up to 573 K. Heating is achieved by wrapping the reactor body with Barnstead Thermolyne standard insulated samox heating tape. Insulation is subsequently wrapped around the heating tape to ensure minimal heat loss and a K-type thermocouple is inserted between the heating tape and the reactor wall. The thermocouple and heating tape are connected to an Omega temperature controller (model #CN2011) capable of operating in a ramp and soak mode for temperature control.

Slurry reactor

A 25ml pyrex erlenmeyer flask with tube in tube metal fitting was used to carry out catalyst screening. The CO_2 gas was bubbled through the mixture for 15 minutes and then the system was pressurized to 20 psig and sealed. The mixture was stirred continuously and exposed to UV light for different duration of time. The liquid products were sampled and analyzed via GC (HP 5890A with 80/100 PORAPAK-Q column) to determine the hydrocarbon composition.

Gas Flow System

The gas flow system is very flexible and allows for both steady-state and transient reaction studies which might utilize any number of gases. The gas flow rates are controlled by Brooks 5850 Series E mass flow controllers. When necessary, pulse injections of one gas into another are achieved by use of a six-port sampling valve and step changes from one gas to another are achieved by use of a four-port step switch valve.

Fig. 6 shows the entire reactor system including the IR cell, light source apparatus, and optical accessories.

Light Source Apparatus

The main components of the light source apparatus include the following: (i) 350 W Hg lamp/lamp power supply/lamp housing, (ii) beam splitter, (iii) 90° beam turner (mirror), (iv) iris diaphragm, (v) UV/visible light filters, (vi) lamp housing, (vii) thermopile detector, (viii) liquid IR filter, (ix) photomultiplier detector, (x) photomultiplier power supply. All items were purchased from Oriel Corporation. Detailed descriptions and function of each item are given in the following subsections.

350 W Hg Lamp/Lamp Power Supply/Lamp Housing

An Oriel 350 W Hg lamp (Model #6286), associated power supply, and housing was used as the source of the UV/visible light. Mercury lamps have a spectrum with many strong lines from 240 to 600 nm, followed by a declining continuum to 2.6 μm.

The Hg lamp is held in place within the lamp housing (Model #66033) and its position can be adjusted such that the optimal amount of light leaves the exit port. A rear reflector is outfitted within the housing opposite the light exit port. This rear reflector collects the back radiation from the lamp and focuses it on or near the arc for collimation by the condenser in order to reflect light that would normally escape toward the exit port, thus increasing output. Total output is up to 60% higher with the reflector. Finally, the condensing lens, located outside the housing at the exit port, consists of a lens element inside a barrel housing with a focusing lever. The condenser is designed to produce a collimated beam, but the focusing lever allows adjustment of the lens position to produce a converging or a diverging beam.

The power supply (Model #68810) is 500 W and is able to maintain output regulation within 1%. This power supply is also equipped with an igniter for easy activation of the light source.

Optical Accessories

The optical accessories include the iris diaphragm, liquid IR filter, UV/visible light filters, beam splitter, and 90° beam turner (mirror). The iris diaphragm (Model #62030) is a variable aperture used for light attenuation. A lever located at the top of the diaphragm controls the aperture. The liquid IR filter (Model #61945) consists of a cell that holds two fused silica windows and an internal chamber that holds distilled water. This filter serves to pass the UV/visible light (250-950 nm) and at the same time remove extraneous IR radiation. Removal of this IR protects the sensitive IR spectrometer and also serves to cool the apparatus. The UV/visible light filters transmit radiation at a desired wavelength, filtering out all other wavelengths.

The beam splitter, called a "Polka Dot" beam splitter (Model #38106), is coated with aluminum with a SiO_2 protective overcoat in a polka dot pattern. The purpose of the beam splitter is to split the incident beam into two beams: one passes through the splitter and the other is reflected 90° from incidence. The reflected beam is sent to detection equipment and the through beam is passed on to the sample.

The beam turner (Model #66215) is a mirror assembly that simply turns the beam 90° from incidence. This is necessary so that the light can irradiate the sample, which is located below the light source.

Calibration

In order to determine the intensity of light striking the reaction sample, a calibration must be performed. This is accomplished with use of a thermopile detector. This detector is first placed the same distance from the light source as the reaction sample and plugged into a sensitive voltmeter or multimeter. Next, several reading are taken on the voltmeter in ambient light and under conditions of irradiation. The readings taken under ambient conditions are averaged and the readings taken under irradiated conditions are averaged. The ambient average is subtracted from the irradiated average, the result is the voltage signal which is proportional to the radiant power falling on the detector, V_s. However, because this detector has only 94% transmittance, the actual value of V_s will be that which was measured divided by 0.94. To compute the radiant power in watts (W), V_s must be divided by the detector's responsivity, R_v. This particular thermopile detector has a responsivity of 9-16 V/W. For calculation purposes, an average value of 12.5 V/W will be assumed. Thus, $W = V_s/R_v$. To compute the irradiance on the detector, H, the radiant power is divided by the detector area (A_d). This area is in units of cm^2. The detector used in this study has an area of 0.04 cm^2. Thus, $H = W/A_d$. For this study, at full spectral irradiance under full power, irradiance was found to be approximately 225 mW/cm^2. By comparison, direct sunlight measured in June in Akron, Ohio gave an irradiance of 49 mW/cm^2. The irradiance of typical sunlight is reported in the literature at 50 mW/cm^2, lending credibility to the accuracy of the thermopile detector.

Analysis Section

The analysis section includes an IR spectrometer, a mass spectrometer, and a gas chromatograph. The IR spectrometer used for these experiments was a 560 Nicolet Magna

equipped with an MCT-B detector at a resolution of 4 cm^{-1}. Typically, 32 scans are coadded to form the spectra.

One of two mass spectrometers was used to monitor gaseous effluent. One MS is a Balzers QMG 112 and the other is a Pfeiffer Prisma QMG 200. In either case, the effluent is fed into a capillary line and into the ionization chanmer, whose operating pressure is a maximum of 1E-6 mbar. The Balzers MS is capable of monitoring eight mass-to-electron (m/e) ratios while the Prisma MS is capable of monitoring up to 64 m/e ratios. Careful selection of the m/e ratios is required to prevent overlapping of the responses as a result of fragmentation in the ionization chamber. Data acquired by the Balzers MS is recorded by an Epson Equity IIe computer while data acquired from the Prisma MS is recorded by a Gateway Pentium computer. Both machines utilize QUADSTAR™ software.

A SRI-8610 gas chromatograph will be used for quantification of both gas and liquid samples. A flame ionization detector was utilized. For liquid hydrocarbon samples, an SE30 column was used and for gas samples, a double Porapak P column was used. The GC is affixed to an integrator for automatic determination of peak areas which, with use of calibration factors, can be converted to concentration.

Catalyst Preparation

Monolayer Ti was prepared by grafting metal precursors, including $Ti(OC_3H_7)_4$ on the surface of Al_2O_3 and Al-MCM-41. Ti precursors was brought in contact with Al_2O_3 or Al-MCM-41 by using a hexane or pentane solution at 300 K. The concentration of metal precursors will be carefully controlled to avoid dimer or trimer formation before grafting. The use of a non-polar solvent will minimize the interface and enhance the interaction between the metal precursors and the surface OH groups.

$$\equiv\text{Si-OH} + \text{Ti}(\text{OC}_3\text{H}_7)_4 \xrightarrow[-\text{HOCH}_3]{} \equiv\text{Si-O-Ti}(\text{OC}_3\text{H}_7)_4$$

$$\xrightarrow[\text{Calcination}]{} \equiv\text{Si-O-TiO or} \equiv\text{Si-O-Ti}$$

Since Al sites on Al-MCM-41 have higher acidity than Si sites, they may preferentially react with OH on Al sites. The monolayer oxide on Al-MCM-41 is expected to be hydrothermally stable. McCullen and Vartuli have found that the post synthesis treatment of as-synthesized MCM-41 with metal alkoxide results in the formation of a metal oxide layer, giving excellent hydrothermal stability up to 973 K with 100% steam.

Al-MCM-41 was prepared by mixing solution A [Tetramethyl amine hydroxide, Cab-O-Sil silica, and H_2O] with solution B [$NaAlO_2$, cetyltrimethylammonium chloride (CTMACl), NaOH, N,N-dimethylhexadecylamine (DMHA), and H_2O]. DMHA was found to be an effective expander. The use of the DMHA/CTMACl ratio of 1 resulted in the large pore (7.7 nm) Al-MCM-41. The mixture was heated in an autoclave under autogeneous pressure at 363 K for 48 hours. Part of the resulting gel was calcined at 773 K for grafting metal precursors; part of gel (as-synthesized Al-MCM-41) was further mixed with Ti precursor solution to initiate the stabilization reaction.

$$\text{Si-O-R} + \text{Ti}(\text{OC}_3\text{H}_7)_4 \rightarrow \text{Si-O-Ti}(\text{OCH}_3)_3 + \text{R-OCH}_3$$

Si-O-R denotes the state of as-synthesized Al-MCM-41 containing R, such as $CTMA^+$, prior to calcination. The resulting sample will be calcined at 773 K to obtain the Ti and Cd-containing Al-MCM-41. The grafting or stabilization reaction may be an effective approach to provide long-term hydrothermal stability as well as unique catalyst activity for photocatalytic synthesis of CH_3OH and hydrocarbons.

RESULTS AND DISCUSSIONS

Methanol formation

Table 1 shows the methanol production rate of TiO_2/SiO_2 and TiO_2/Al_2O_3 in slurry reactor. Monolayer TiO_2 dispersed on Alumina exhibited higher activity for methanol formation compared to TiO_2 on silica while TiO_2/MCM-41 doesn't show any activity for methanol production.

Catalyst	Time (h)	CH_3OH conc. (µmol/µl)	Reaction rate (µmol/h -g cat)
TiO_2/SiO_2	30	9.2 e-02	6.1 e-04
TiO_2/Al_2O_3	1	2.9 e-02	5.8 e-03
	5	7.0 e-02	2.8 e-03

Table 1: Product analysis of slurry reaction mixture

Light intensity through Erlenmeyer flask

Table 2 below shows the light intensity measured through the flask at different angles and distance from light source. Pyrex glass is opaque below 280 nm and doesn't transmit 100% of UV radiation. Moreover, the orientation of erlenmeyer flask due to its concave and convex curvature affects intensity of light incident on the slurry reaction mixture. To avoid the complications associated with this reactor, a quartz reactor with a flat surface perpendicular to incident light is designed as shown in Fig. 7**.**

Diagram	Intensity (mV) and Distance 3.125 in	Intensity (mV) and Distance 6.25 in
	41.5	19.5

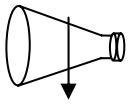	24.7	13
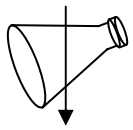	25.7	13.4

Table 2: U.V. Light Intensities at 25 mL E-Flask Angle and distance

Combinatory optical fiber approach

A combinatorial study for catalyst screening is planned by designing a set of reactor with optical fibers. A fiber optic bundle with multiple legs would be connected to the UV light source with an interface. Each high fused silica optical fiber leg will be 3.1 mm OD and have 55% UV transmittance. Figure 8 shows the design of combinatory reactors with fiber optics.

CONCLUSION

We have design and constructed three reactor system: (i) IR cell for catalyst preparation (ii) IR cell for monitoring adsorbed species during photocatalytic reaction, and (iii) flask reactor for catalyst screening studies. The results of year 1 studies show that monolayer TiOx may be further modified to enhance its activity for photocatalytic reduction of CO_2/H_2O to methane and methanol.

REFERENCES

1. H. Herzog, E. Drake, and E. Adams, *in* "CO_2 Capture, Reuse, and Storage technologies for Migrating Global Climate Change", DOE Order No: DE-AF-22-96PC01257.
2. M. Anpo, *in* "Surface Photochemistry", John Wiley and Sons, New York 1995.
3. C. Kutal, N. Sepone, in "Photosensitive Metal-Organic System", Advances in Chemistry Series 238, American Chemical Society, Washington DC, 1993.
4. M. Anpo, H. Yamashita, Y. Ichihashi, Y. Fujii, M. Honda, *J. Phys. Chem.:B* **101**, 2632-2636 (1997).
5. M. Anpo, S. G. Zhang, Y. Fujii, Y. Ichihashi, H. Yamashita, K. Koyano, T. Tatsumi, *in* "The Photocatalysis Reduction of CO_2 with H_2O on Ti-MCM-41 and Ti-MCM-48 Mesoporous Zeolite Catalysts at 295 K", Apcat'97, Pohang University, Korea, 1997.
6. A.L. Linsbigler, G. Lu, and J.T. Yates Jr., *Chem. Rev.* **95**, 735 (1995).
7. M. Voinov, and J. Augustynski, *in* "Heterogeneous Photocatalysis", (M. Schiavello Ed.), Photoscience and Photoengineering, Vol. 3., p. 1. Wiley, New York, 1997.
8. M. Tanaka, *in* "Photochemistry on Solid Surfaces" (M. Anpo and T. Matsura, Eds.), Studies in Surface Science and Catalysis, Vol. 47, p. 3. Elsevier, New York, 1989.
9. L. Palmisano, and A. Sclafani, *in* "Heterogeneous Photocatalysis", (M. Schiavello Ed.), Photoscience and Photoengineering, Vol. 3., p. 109. Wiley, New York, 1997.
10. S. Yanagida, S. Matsuoka, M. Kanemoto, K. Yamamoto, K. I. Ishihara, T. Ogata, and Y.Wada, *in* "Research in Photosynthesis", 9th International Congress on Photosynthesis, Vol. II, p. 833. Kluwer, Boston, 1992.

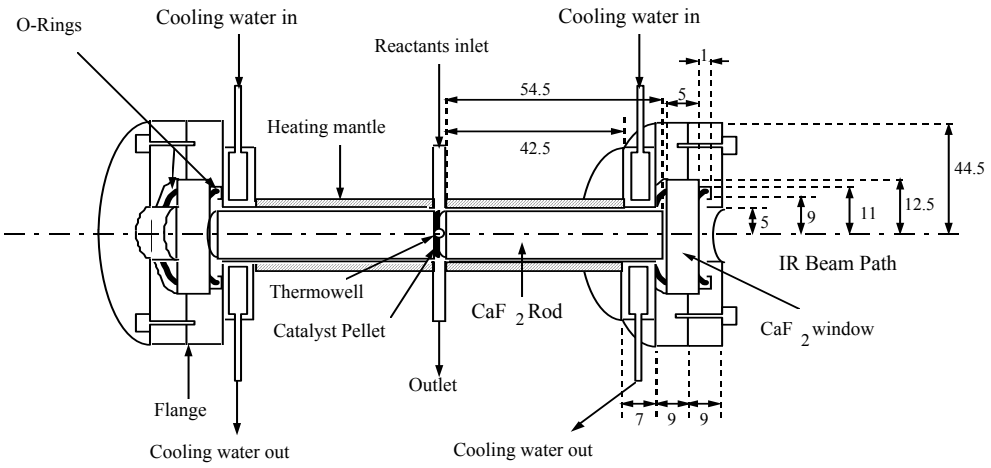

Note: All dimensions are in mm.

Fig. 1. Transmission IR cell

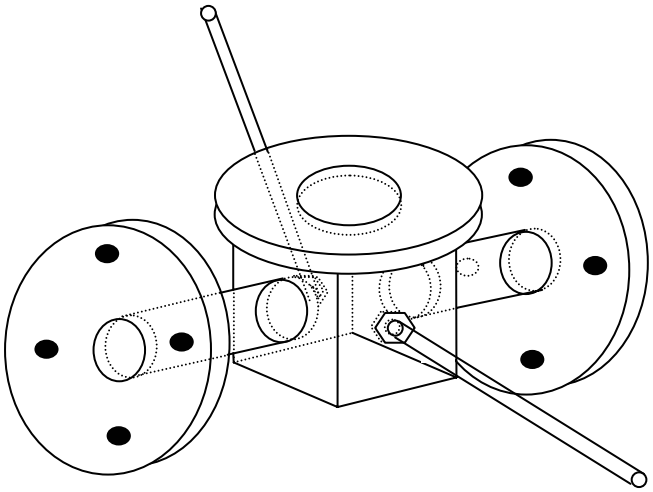

Fig. 2. Photocatalysis reactor

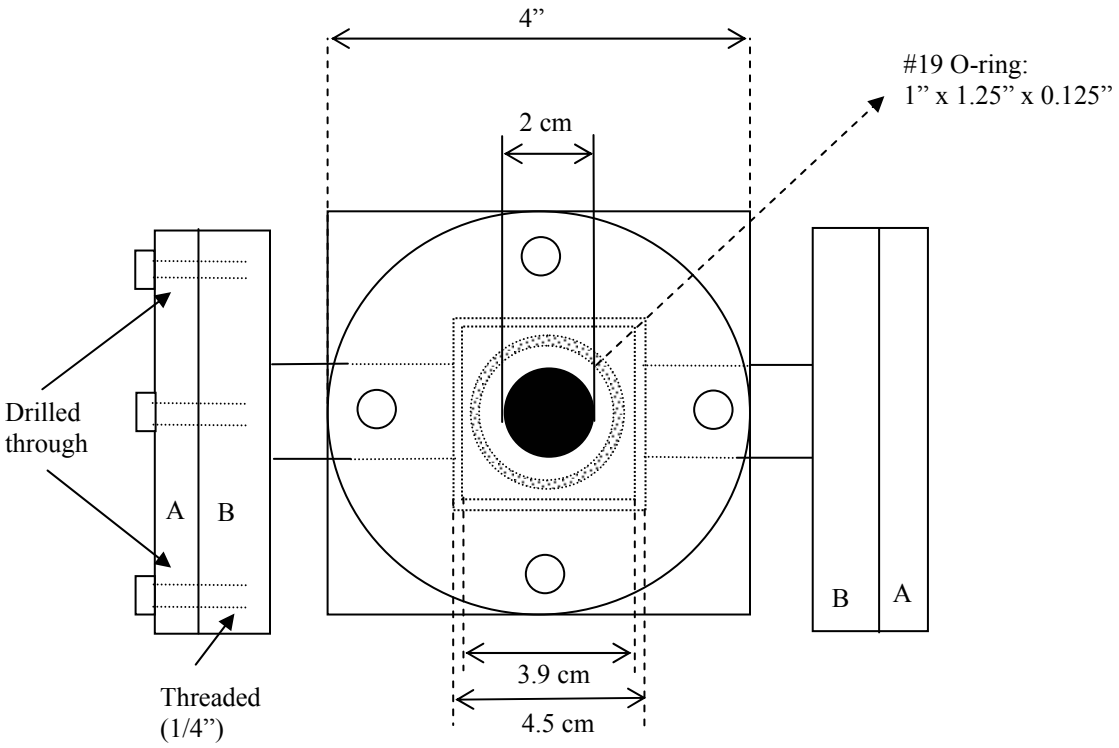

Fig. 3. High-Pressure Photoreactor (Top View)

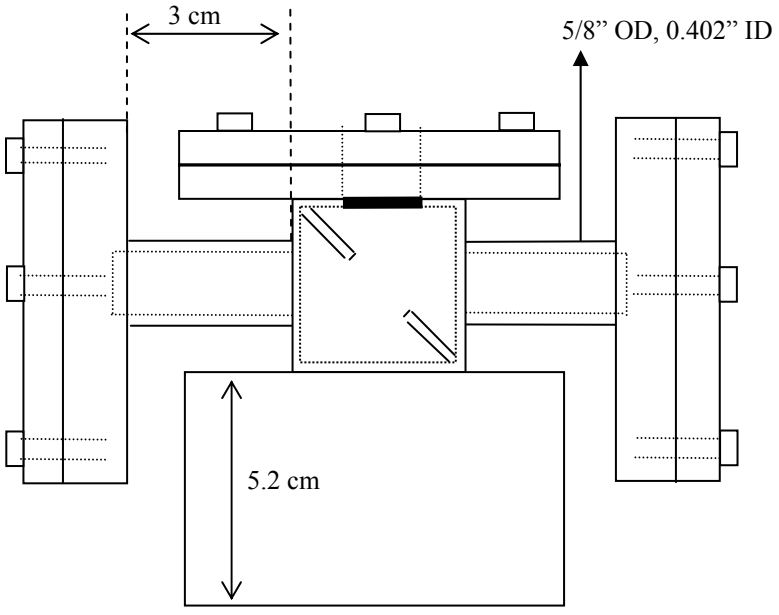

Fig. 4. High-Pressure Photoreactor (Side View)

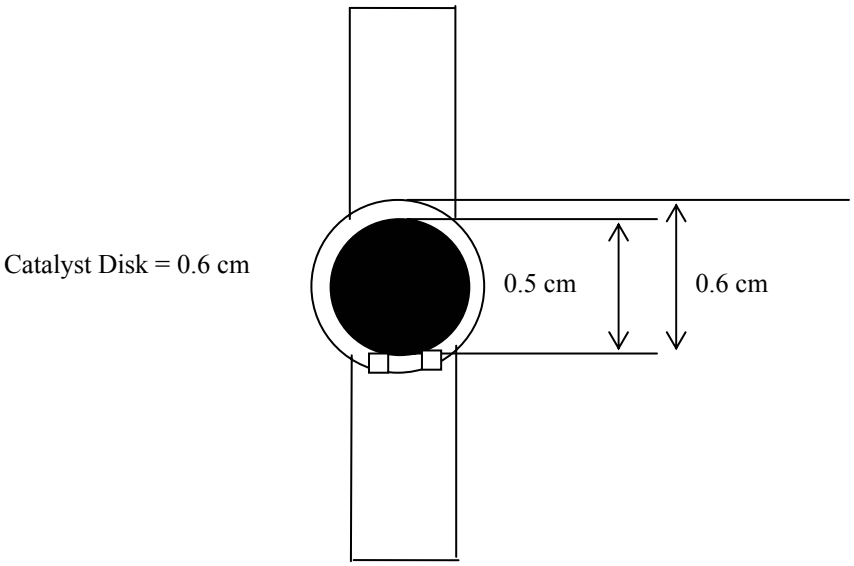

Fig. 5. Catalyst Holder

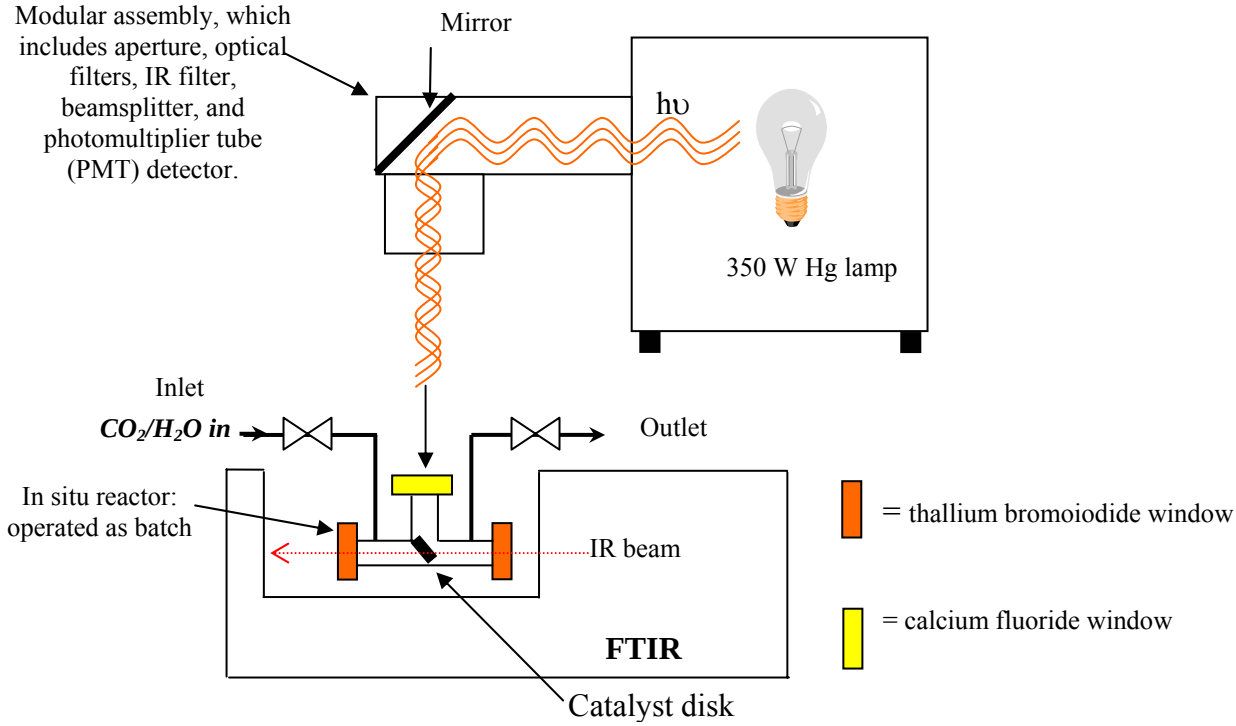

Component	***Function***
Aperture	Tunes energy intensity
Optical filter	Tune wave length
IR filter	Removes extraneous IR radiation
Beamsplitter reactor	Splits beam path between PMT and reactor
PMT detector	Allows monitoring and quantification of light intensity

Fig. 6. Experimental apparatus.